Individual growth rate (IGR) and aminoacyl-tRNA synthetases (AARS) activity as individual-based indicators of growth rate of North Pacific krill, *Euphausia pacifica*

Anna K. McLaskey [a1*], Julie E. Keister[a], Lidia Yebra[b]

[a]School of Oceanography, University of Washington, Seattle, WA 98105, USA

[b]Instituto Español de Oceanografía, Centro Oceanográfico de Málaga, 29640, Fuengirola, Málaga, Spain

* corresponding author: a.mclaskey@oceans.ubc.ca

[1] Present address: Institute for the Oceans and Fisheries, University of British Columbia, Vancouver, BC, V6T1Z4, Canada

Abstract

We investigated aminoacyl-tRNA synthetases (AARS) activity and individual growth rate (IGR) as individual-based *in situ* indicators of growth in adult krill, *Euphausia pacifica*. Growth rates of field-collected krill were measured via the IGR method and individuals were subsequently preserved for AARS analysis to yield paired measurements. Our results show that conditions during the IGR incubation period influenced AARS activity in these individuals precluding a direct comparison but revealing the different timescales across which these two measures integrate. Importantly, they show that AARS activity provides a snap-shot image of an organism's metabolism, while IGR of krill is thought to integrate their environmental experience over several days. Each method would require repeated measurements to estimate population growth rates integrated over seasonal or generational time scales. As part of this project, we investigated how specific the AARS assay is to protein synthesis by testing a modified protocol that includes an additional blank and found evidence that the current assay may be measuring other cellular processes in addition to its intended signal. Our results suggest that a new NADH Blank might be optimized to improve the specificity of the assay.

1. Introduction

The growth rate of zooplankton is an important parameter for understanding their role in marine ecosystems, such as determining zooplankton production and biogeochemical cycling, but is extremely difficult to estimate *in situ* (Kobari et al., 2019). Methods to estimate zooplankton growth rates include cohort analysis methods, incubation techniques, models, and biochemical indices of, e.g., nucleic acid, protein, and chitin production. Each of these methods includes assumptions and drawbacks, and may be useful in some situations but not others. Of

these options, biochemical methods tend to be simple and quick, allowing for broad scale sampling, and therefore are becoming more widely used (Yebra et al*.,* 2017).

Krill are key components of many marine ecosystems, linking primary production to higher trophic levels (Mauchline and Fisher, 1969). Measurements of their growth rate are critical to estimating zooplankton production in these systems and for understanding their population dynamics and responses to environmental conditions. The individual growth rate (IGR) method was developed specifically for krill as an alternative to the natural cohort technique (Quetin and Ross, 1991; Nicol et al., 1992; Ross et al., 2000) and estimates growth rate by incubating individuals for a few days, then measuring the change between the length of any shed exoskeletons and the length of the animal after molting. Combined with an overall molting rate from the experiment, this individual growth increment is used to estimate growth rate. The method assumes that the growth increment reflects *in situ* conditions experienced by the individual during the inter-molt period, and that the number of individuals molting is relatively constant over time and not affected by incubation conditions. The approach has been used in studies of the Antarctic krill, *Euphausia superba* (e.g., Ross et al., 2000; Nicol, 2000; Atkinson et al., 2006; Tarling et al., 2006), and Pacific krill, *E. pacifica* (Pinchuk and Hopcroft, 2007; Shaw et al., 2010).

Aminoacyl-tRNA synthetases (AARS) are a group of enzymes that catalyze the aminoacylation of tRNA, the first step of protein synthesis. Their activity is directly related to protein synthesis and has been developed as a proxy for growth rate in zooplankton (Yebra and Hernández-León, 2004; Yebra et al., 2011; 2017). Methods for measuring the activity of individual AARS enzymes, or multiple AARS enzymes, often use radio-labeled ATP (Boniecki et al., 2008) or amino acids (Awai et al., 2015) to measure activity. These assays are complicated

and require the addition of tRNA for each AARS enzyme, as well as its corresponding amino acid. A continuous colorimetric assay has also been developed to measure AARS activity based on the release of pyrophosphate (PPi) during the aminoacylation of tRNA (Chang et al., 1984). This initial method included the addition of substrates (tRNA and amino acids) but since then, a simplified version of the assay has been developed without the addition of substrates (Yebra and Hernández-León, 2004). This simplified method uses a commercial PPi detection kit (Sigma P7275) that contains a pyrophosphate-dependent fructose-6-phosphate kinase (PPi-PFK), which catalyzes the first of four coupled reactions that ultimately result in oxidation of β-nicotinamide adenine dinucleotide (NADH). The oxidation of NADH is then measured as the change in absorbance at 340 nm over time, and is converted to the rate of PPi released.

AARS activity is a broadly applied method that has been measured in several crustacean zooplankton taxa and calibrated with other direct (length, dry weight, protein variations) and indirect (egg production, RNA:DNA, empirical models) estimates of growth (e.g., Guerra 2006; Herrera et al., 2012; Holmborn et al., 2009; Yebra and Hernández-León, 2004; Yebra et al., 2005; 2006; 2011).

The commercial PPi detection kit used for the AARS assay contains a PPi-dependent enzyme to couple PPi to NADH oxidation, but there are other compounds present in a homogenized zooplankton sample that can also oxidize NADH. The commercial Pyrophosphate Reagent also includes a high concentration of NADH, which would cause a large change in redox state and likely stimulate different reactions in the sample homogenate. The current methodology uses a blank that contains the Pyrophosphate Reagent and water without the addition of sample homogenate, and therefore measures NADH oxidation due to the non-enzymatic background oxidation associated with the reagent mixture. Potential NADH oxidation

due to other compounds in the zooplankton sample cannot be separated with the current methodology.

In this study, we sought to investigate AARS activity and IGR in adult *E. pacifica* and to explore methodological advantages and constraints of each. Another goal was to assess how specific the AARS assay is to protein synthesis by testing a modified protocol with an additional blank. This study was part of a larger project that performed AARS activity and NADH oxidation tests in more individuals than IGR; electron transport system (ETS) activity was also measured, providing additional physiological information.

2. Methods

We conducted two cruises, 23-30 June and 25 Aug-1 Sept 2018, aboard the R/V Clifford A. Barnes in Puget Sound, Washington, USA. Live adult female *E. pacifica* were collected from surface waters (upper 50 m) at each of four sampling stations (Fig. 1) during the nighttime using a 60-cm diameter Bongo frame equipped with black 335-µm mesh nets and non-filtering cod ends towed for less than 10 min. The contents of each cod end were diluted in coolers of seawater and immediately sorted for healthy euphausiids. Adult euphausiids were identified under a microscope and healthy adult females (with obvious ovaries) were separated to use in IGR experiments at a subset of stations (Table 1). From three stations, additional individuals were also frozen on liquid nitrogen for enzymatic analyses (described below) immediately after sorting.

Table 1. Summary of IGR experiments. Cruise and station of krill collection, protein specific AARS activity (spAARS; nmol PPi mg protein^{-1} hr^{-1}), weight specific growth rate (Wt sp GR; d^{-}

110 ^{1}), growth rate (mm d^{-1}), inter-molt period (IMP; d), number of individuals (n Ind.), measured
111 total length post-molting (TL; mm), full water column depth integrated temperature (Temp; ˚C),
112 0-30 m depth integrated Chl *a* (µg L^{-1}), and bottom depth (m) at each station location. Average
113 values and standard error given for individual-based measurements. Superscript letters indicate
114 statistically significant differences in responses among experiments.

Cruise	Station	spAARS ±1 S.E.	Wt sp GR (day^{-1}) ±1 S.E.	Growth rate ±1 S.E.	IMP	n Ind.	TL ±1 S.E.	Temp (˚C)	Chl a 0-30 m (µg L^{-1})	Bottom depth (m)
June	P12	103 ± 18 ^{ab}	0.015 ± 0.004 ^{a}	0.064 ± 0.02 ^{a}	4.8	11	15.7 ± 0.8 ^{a}	9.8	5.08	130
August	P11	66 ± 11 ^{bc}	0.003 ± 0.002 ^{bc}	0.013 ± 0.01 ^{b}	14	6	16.2 ± 0.4 ^{a}	10.2	3.16	89
August	P12	61 ± 3 ^{c}	0.009 ± 0.002 ^{ab}	0.041 ± 0.01 ^{ab}	8.4	11	15.8 ± 0.3 ^{a}	10.2	1.91	130
August	P8	113 ± 17 ^{a}	0.002 ± 0.002 ^{cd}	0.012 ± 0.01 ^{a}	8.2	9	18.7 ± 0.3 ^{b}	11.8	1.68	132
August	P38	65 ± 5 ^{bc}	0.006 ± 0.002 ^{bd}	0.030 ± 0.01 ^{a}	7.7	10	17.9 ± 0.3 ^{b}	13.6	1.90	101

115

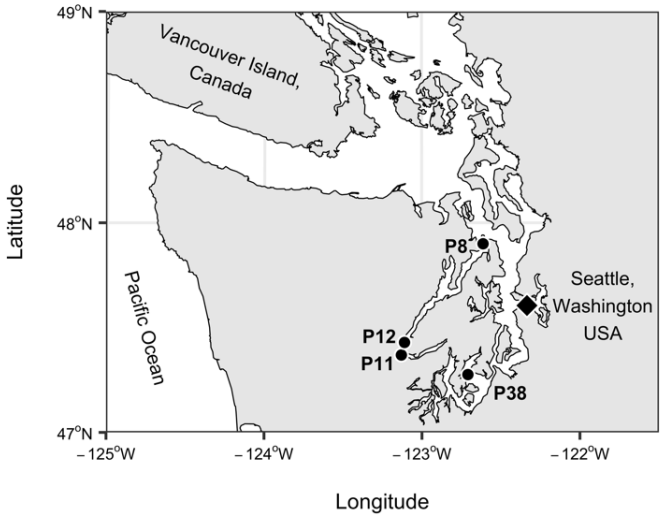

116

117 Fig. 1. Sampling locations in Puget Sound, Washington, USA.

118

119 ## 2.1. Individual Growth Rate Experiments

In each individual growth rate (IGR) experiment, adult female *E. pacifica* were added one per 500-mL jar of 200-μm filtered seawater then incubated at 12 ˚C in the dark for 48 h following the methods of Shaw et al. (2010). Five experiments were run with 30-50 individuals each. Jars were checked for molts under red light every 12 h and individuals that had molted were removed along with their shed exoskeleton. We measured telson length of both the exoskeleton and the animal, as well as total length of the animal; all measurements were conducted by the same person at 6X magnification for total length and 25X for telson lengths using a calibrated eyepiece reticle. Krill were kept at experimental temperature until measuring, which was done in less than one minute, then individuals were flash frozen alive in liquid nitrogen for enzyme analyses (described below) and stored at -70 ˚C until they were processed (max. 9 months later).

Telson lengths were converted to total length (TL) according to the equation TL (mm) = 4.937*telson length (mm) – 0.4142 (Shaw et al., 2010). The growth increment was defined as the difference between the total length calculated from the animal's telson length and total length calculated from the exoskeleton telson length.

Inter-molt period (IMP) was calculated after Tarling et al., (2006) according to the equation IMP=N*d/m where N is the number alive at the end of the experiment plus the number that had molted and been removed during the experiment, m is the number that molted, and d is the length of the incubation in days.

Growth rate (g) of each individual was calculated by dividing the growth increment by the inter-molt period; weight specific growth rates were calculated by converting TL to dry weight and assuming carbon weight (W) was 40% of dry weight using a published length-weight regression (Feinberg et al., 2007).

$$g = \frac{\ln\left(\frac{Wpostmolt}{Wpremolt}\right)}{IMP} \quad (\text{day}^{-1}) \qquad (1)$$

2.2 Enzyme Analyses

Samples were removed from the -70 ˚C freezer, immediately ground with a Teflon glass grinder at 2 ˚C for 90 sec in 20-mM Tris Buffer (pH 7.8), then centrifuged at 4000 rpm for 10 min at 2 ˚C. We then used aliquots of the supernatant to assay AARS activity, protein concentration, and electron transport system (ETS) activity. The AARS activity assay was run on a total of 112 individual adult female *E. pacifica*; an NADH Blank (described below) was also run on each.

To test whether a significant component of the NADH oxidation detected by the AARS assay is due to redox reactions stimulated by the change in redox state rather than by the release of PPi during aminoacylation, we measured the activity in cell homogenate two ways: 1) with the addition of the full Pyrophosphate Reagent and 2) with the addition of 0.8 mM NADH in 45 mM Imidazole buffer (pH 7.4), two of the components of the Pyrophosphate Reagent (Table 2), which hereafter we will call an NADH Blank. Although a full mixture containing all the components of the Sigma® Pyrophosphate Reagent except the PPi-dependent PFK would be the ideal blank to test, it is a complex proprietary mixture, and we aimed to test the stimulated NADH oxidation due to the addition of NADH alone.

Table 2. Components and final concentrations of Sigma® P7275 Pyrophosphate Reagent. Italics indicate components of the NADH Blank.

Component	Concentration
Imidazole ・HCL, pH 7.4	*45 mM*

Citrate	5 mM
EDTA	0.10 mM
Mg^{2+}, Mn^{2+}, Co^{2+}	2 mM, 0.2 mM, 0.02 mM
β-NADH	*0.8 mM*
D-Fructose-6-phosphate	12 mM
Bovine Serum Albumin	5 mg/ml
Sugar Stabilizer	5 mg/ml
Fructose-6-phosphate kinase, pyrophosphate dependent (PPi-PFK)	0.5 units/ml
Adolase	7.5 units/ml
Glycerophosphate dehydrogenase	5 units/ml
Triosephosphate isomerase	50 units/ml

AARS was measured following the method of Yebra and Hernández-León (2004), modified by Yebra et al. (2011), and adapted for a 96-well plate (Yebra et al., 2017). Assays contained 60 µL of water, 40 µL of Pyrophosphate Reagent (Sigma P7275), and were initiated with the addition of 50 µL of sample supernatant. NADH Blanks contained 60 µL of water, 40 µL of 0.8-mM NADH in 45-mM Imidazole buffer (pH 7.4), and 50 µL of sample supernatant. For each sample, assays and NADH Blanks were measured in triplicate. In addition, during each run two types of background blanks were run in triplicate: PPi reagent background (equivalent to blank assay in Yebra and Hernández-León 2004) containing 60 µL of water, 40 µL of Pyrophosphate Reagent (Sigma P7275), and 50 µL of 20mM Tris Buffer (pH 7.8); and NADH background containing 60 µL of water, 40 µL of 0.8 mM NADH in 45 mM Imidazole buffer (pH 7.4), and 50 µL of 20 mM Tris Buffer (pH 7.8) (one sample assay is shown in Fig. S1 as an example).

Oxidation of NADH was monitored for 15 min at 25 ˚C by the decrease in absorbance at 340 nm with a spectrophotometer (SpectraMax M2, Molecular Devices). AARS activities were calculated as in Herrera et al. (2017) and corrected to *in situ* temperatures with the Arrhenius equation using an activation energy of 8.57 kcal mol^{-1} (Yebra et al., 2005). In addition, we

calculated AARS activity subtracting the NADH blank to correct the assay activity. First the background blanks were accounted for, then the slope of the NADH Blank was subtracted from the Assay slope (Eq. 2).

$$(\Delta\text{AARS Assay} - \Delta\text{PPi reagent background}) - (\Delta\text{NADH Blank} - \Delta\text{NADH background}) \quad (2)$$

2.2.1. Protein content

Protein content was determined according to the bicinchoninic acid (BCA) method (Smith et al., 1985) using a Pierce BCA Protein Assay Kit (Thermo Scientific). Sample supernatant was diluted to 1/16 concentration with Tris buffer to target a protein concentration of 25-250 mg mL^{-1}, within the linear range of this assay. Bovine serum albumin was used as a standard and dilutions were prepared using Tris buffer. Triplicate assays were run for each sample.

2.2.2 Electron transport system (ETS) activity

As part of a larger project, electron transport system (ETS) activity was also measured in the individual krill. ETS was assayed using the method of Owens and King (1975), as modified by Gómez et al. (1996), and adapted for a 96-well plate. ETS activity was measured via INT (2-(p-iodophenyl)-3-(p-nitrophenyl)-5-phenyl tetrazolium chloride) reduction to formazan for 12 min by the increase in absorbance at 490 nm with a spectrophotometer (SpectraMax M2, Molecular Devices). For each assay, 30 µL of sample supernatant were added to 90 µL substrate solution (1.7 mM NADH and 0.25 mM NADPH dissolved in phosphate buffer) and the reaction was initiated by adding 30 µL INT (0.2%, pH 8.5). Blank measurements were taken using phosphate buffer (0.1M phosphate buffer pH 8.5, 0.2% v/v triton x-100, 0.15% w/v polyvinylpyrrolidone, 75 µm $MgSO_4$) without added substrates. Assays and blanks were

measured in triplicate at 25 ˚C, calculated according to Packard and Christensen (2004), and corrected to *in situ* temperatures using the Arrhenius equation with an activation energy of 15 kcal mol^{-1} (Packard et al., 1975).

2.3 Statistical Analysis

Factors that influence IGR-estimated growth rate and spAARS activity among individual krill were investigated using linear models in R (V. 3.5.2) with the best model determined based on AICc using the package AICcmodavg. Total length (post-molt), calculated dry weight, assayed protein content, full water column depth integrated temperature at collection station, 0-30 m integrated Chl *a* at collection station, and time to molt (12, 24, 36, or 48 hrs) were included as fixed effects. We checked residual plots for homoscedasticity and normality; spAARS was log transformed to meet model assumptions. The relationship between IGR-estimated growth rate and spAARS activity was tested with a linear model. Differences in spETS and log(spAARS) activity among individuals immediately frozen in the field and those used in IGR experiments were tested with linear mixed models (lme4 package) that included the collection location as a random effect and Before/After incubation as a fixed effect.

To assess the processes driving activity in the NADH Blank of all krill analyzed in the larger project (n=112), the activity was log transformed and treated as the response variable (one sample with a negative NADH Blank due to low activity and a high background blank was removed). The activity of the AARS Assay was also log transformed and considered as a fixed effect along with dry weight, ETS activity (μmol O_2 hr^{-1}), and collection station. One process that could potentially contribute to the oxidation of NADH separately from protein synthesis is

the electron transport system; because ETS activity was also assayed on the same individual krill in this project, it was included in the analysis as an explanatory variable.

3. Results

3.1 IGR-estimated growth rate and AARS activity

The five IGR experiments resulted in 47 individuals that molted and provided good measurements of both the molt and the post-molt individual (Table 1). Their sizes ranged from 13.7-21.5 mm total length (16.8 ± 1.88; mean ± standard deviation). Inter-molt period (IMP) among the five experiments ranged from 4.8-14 days and averaged 8.6 ± 3.3 days. Growth increments ranged from -0.296 to 0.69 mm (0.24±0.24), growth rates from -0.038 to 0.134 mm d^{-1} (0.03±0.04), and -0.007 to 0.034 d^{-1} (0.008±0.009).

The best model describing IGR-estimated growth rate included total length, field Chl *a*, and time to molt as predictors (S1 Table). Weight specific growth rate decreased with increasing total length (Figure 2a; $p<0.001$, $R^2=0.28$) and similar relationships were observed for growth rate (mm day^{-1}), weight specific growth rate (day^{-1}), and growth increment (mm), as compared to measured total length, calculated dry weight, and assayed protein concentration.

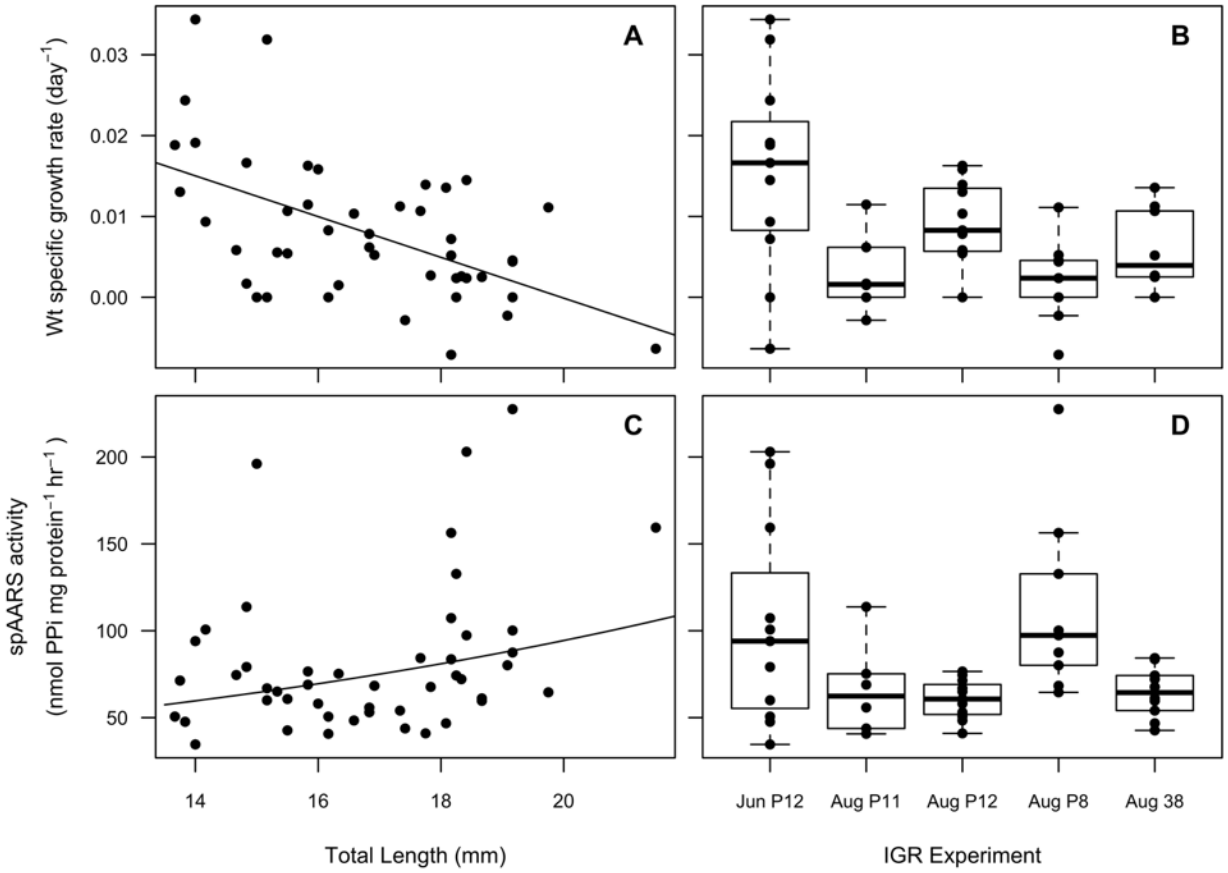

Fig. 2. (A) Weight specific growth rate (d^{-1}) measured by the individual growth rate (IGR) method compared to measured post-molt total length (mm), with solid line showing the total length model estimate. (B) Weight specific growth rate among the five different IGR experiments; bold line indicates the median, boxes show the inter-quartile range, dashed lines show the range of data, and points show the measurements from each individual. (C) spAARS (nmol PPi mg protein^{-1} hr^{-1}) activity versus measured post-molt total length (mm), with solid line showing the log(spAARS) total length model estimate. (D) spAARS activity among the five different IGR experiments.

AARS assay activity in these 47 individuals ranged from 45 to 529 nmol PPi hr^{-1} (152 ± 110) and spAARS activity ranged from 35 to 228 nmol PPi mg protein^{-1} hr^{-1} (82 ± 43). Four

models had AICc scores within 2 of each other and all four included total length as a predictor variable; the best also included Chl *a*, while the others included temperature; both Chl *a* and time to molt; or no other factors besides total length (S1 Table). Log transformed spAARS activity had a weak but significant positive relationship with increasing post-molt total length (Fig 2c; $p=0.02$, $R^2=0.09$). Weight specific growth rate (d^{-1}) was not correlated with enzyme activities after incubation (Fig 3), while growth increment was very weakly negatively correlated with spAARS activity ($p=0.02$, $R^2=0.09$).

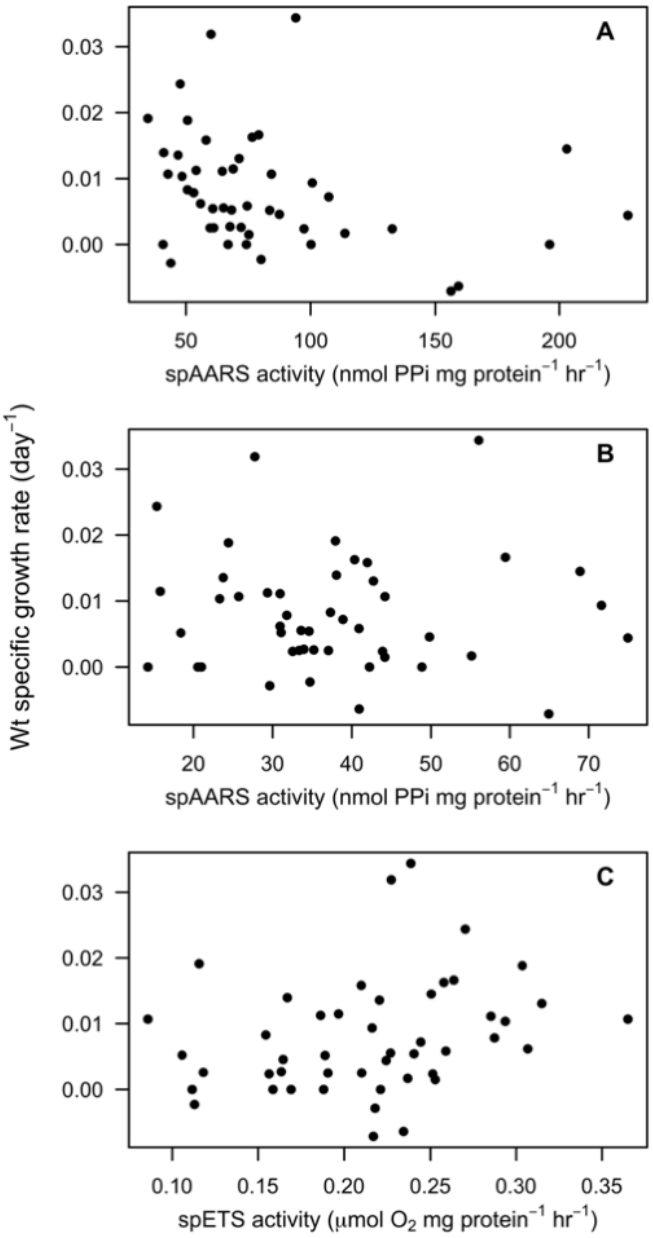

262

263 Fig. 3. IGR-measured weight specific growth rate compared to enzyme activities measured in the
264 same individuals after 12-48 h starvation. IGR-estimated growth rate versus (A) spAARS with
265 PPi reagent background blank correction (R^2=0.06, p=0.06, (B) spAARS with NADH Blank
266 correction (R^2<0.01, p=0.84), and (C) spETS activity (R^2=0.05, p=0.07).

267

268 The effect of IGR incubation period on spAARS and spETS was tested with data from
269 the three stations where some individuals were immediately frozen in liquid nitrogen in addition
270 to those used in IGR experiments. The best model for log(spAARS) included station as a random
271 effect and Before/After incubation as a fixed effect (Fig 4; S2 Table). Those that were frozen
272 immediately, without an incubation period, generally had lower and less variable spAARS
273 activity than those that were preserved after the 12-48 hour IGR incubation period. The best
274 model for spETS activity only included station as a random effect and not Before/After
275 incubation (Fig 4; S2 Table).
276

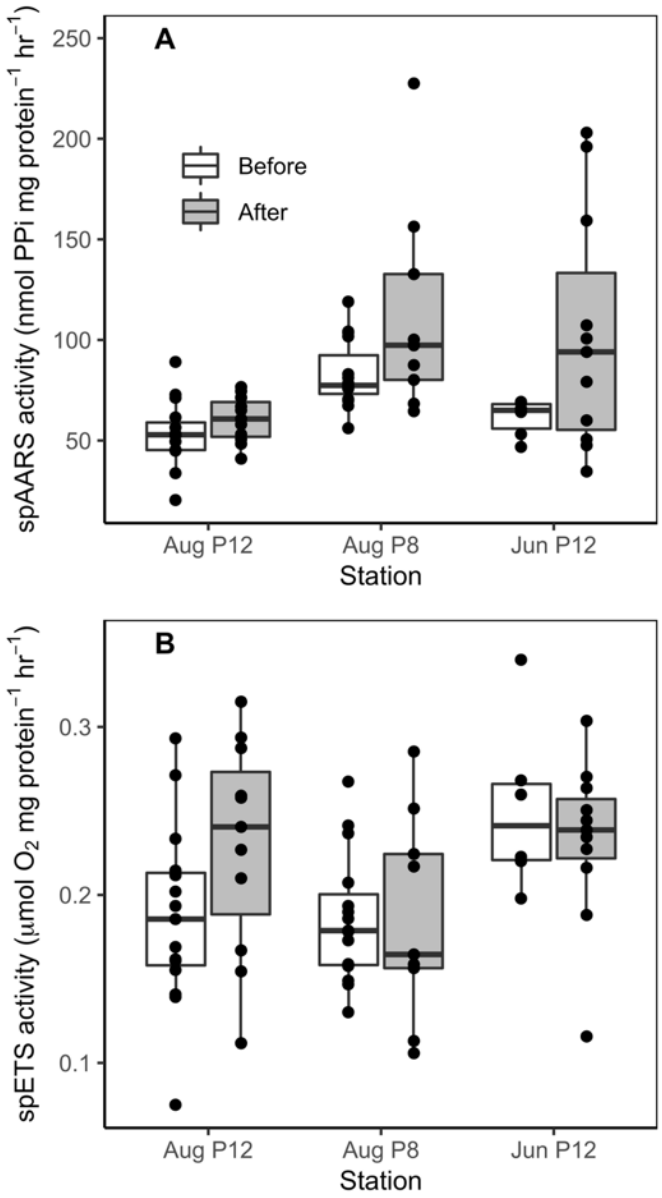

277

278 Fig. 4. (A) spAARS and (B) spETS activities in adult female *E. pacifica* that were flash frozen
279 immediately after capture (white bars) and that were collected from the same station but
280 incubated for 12-48 hours in IGR experiments (grey bars). Boxes show the inter-quartile range,
281 bold horizontal line indicates the median, vertical lines show the range of data, and points show
282 the measurements from each individual.

283

3.2. NADH oxidation

Significant changes in absorbance were observed in NADH Blanks for all samples, and the slope of the Blanks was closely correlated with the slope of the AARS Assays (R^2=0.85, $p<0.001$, Fig 5). The activity detected in the NADH Blanks ranged from -0.1 to 93% (mean 50% ±17% SD) of the activity when the Pyrophosphate Reagent was added. The best model of log(NADH Blank slope) included log(Assay slope) and ETS activity, but not dry weight or collection station (S3 Table). Three other models had AIC scores within 2 of the top model, each containing log(Assay) either on its own, with dry weight, or with dry weight and ETS activity (S3 Table).

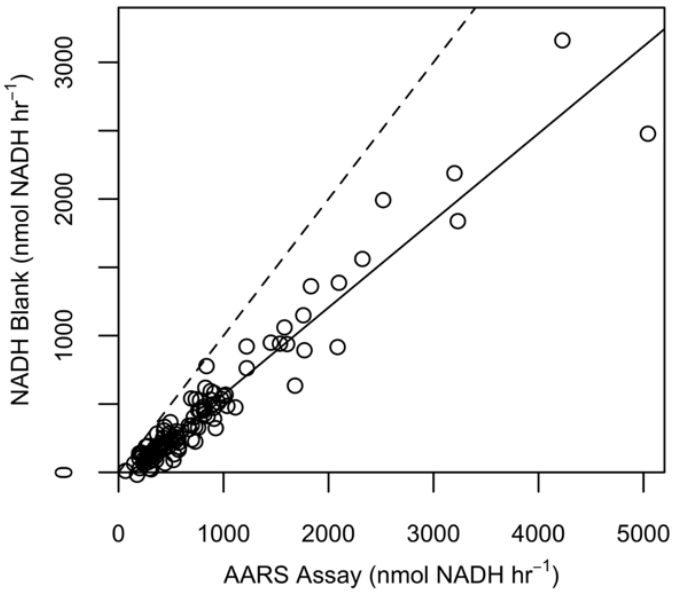

Fig. 5. Activity measured in NADH Blanks (nmol NADH hr^{-1}) versus activity measured in the AARS Assays (nmol NADH hr^{-1}) after correction with each corresponding background blank (log-log regression R^2=0.85, $p<0.001$). Regression line shown as solid line; 1:1 line is dashed.

When the assay activity was corrected using the additional NADH blank, log(spAARS) activity showed no relationship with dry weight (R^2=0.04, p=0.18, not shown) and IGR-estimated weight specific growth rate showed no relationship with spAARS (Fig 3b; R^2<0.01, p=0.84). IGR-estimated weight specific growth rate was also not correlated with spETS activity (Fig 3c; R^2=0.05, p=0.07).

4. Discussion

Our data show differences in IGR and AARS activity in individual adult female *E. pacifica* that likely resulted from the different time scales over which these two measures integrate and the degree to which they were influenced by the incubation period. IGR was best explained by individual total length, time to molt, and chlorophyll concentration in the field, while spAARS activity was best explained by individual total length. We also found evidence that the AARS assay may be measuring other processes in addition to the PPi-producing aminoacylation reactions: significant NADH oxidation was observed in all samples to which only NADH had been added, which suggests additional, unidentified processes contributed to the assay signal.

Crustaceans accommodate growth by molting, so changes in length occur as discrete events while changes in weight occur continuously. The IGR method measures these discrete length increases and therefore must estimate mass from length using established relationships. A key assumption of the method is that growth increment is set by environmental conditions prior to when the krill are collected and is not influenced by incubation conditions, but there is evidence that growth increment can decrease during incubation under food limited conditions (Tarling et al., 2006). While a key benefit of the IGR method is obtaining growth measurements

from individuals, the overall molting rate from the experiment is used to estimate a growth rate, which assumes a constant molting rate of the population. AARS activity indexes protein synthesis, a continuous process linked to changes in mass. The rate at which AARS activity in zooplankton changes is not well constrained, but it responds to food concentrations within 24-48 hours in copepods (Holmborn et al., 2009), and *E. distinguenda* displays diel variability in both AARS and ETS activities (Herrera et al., 2019).

Our data further support that AARS activity changes on time scales of less than 48 hours. Individuals that were immediately frozen in the field had lower and less variable spAARS activity than those that were used in IGR experiments, revealing the influence of the IGR incubation period on spAARS activity. The increase in spAARS was most likely due to starvation during incubation, which causes organisms to burn their own lipids and proteins to fuel basal metabolism (Ikeda, 1977). This would decrease individual biomass and elevate their protein-specific AARS activity because protein synthesis rates include protein turnover (e.g., recycling of muscle, enzymes, nucleic acids, etc.) in addition to somatic growth. ETS activity in the same individuals did not differ between capture and post-incubation. ETS activity was likely less influenced by starvation because it is measured with the addition of saturating substrates**.** Its activity depends on the number of enzymes in the organism's cells rather than also on the concentration of endogenous substrates in the cells at the time of capture. On the other hand, AARS activity is sensitive to both the concentration of endogenous substrates and of active enzymes in the cells, which are determined by the length of the starvation period and the physiological status of the organisms prior to incubation. It is also possible that catabolism of proteins under starvation increased the concentration of substrates and increased AARS activity. These changes likely emerge shortly after transfer into food limited conditions. The current study

345 was part of a larger project that related AARS activities to environmental conditions which found
346 that when individuals were immediately frozen, AARS activity was correlated with
347 environmental drivers, but when they were held in filtered seawater for 2-3 hours before
348 freezing, no relationships were evident (Mclaskey 2019; McLaskey and Keister, *unpublished*).
349 Low food conditions can lead to negative relationships between spAARS and growth
350 rate, potentially due to degradation of proteins during starvation or ß-oxidation of fatty acids that
351 also produces PPi, so would increase spAARS activity (Herrera et al., 2012). Lipids play an
352 important role in krill energetics and egg production, so lipid catabolism was likely occurring in
353 the mature females used in this study. Food conditions are rarely optimal in the field and can
354 fluctuate widely on daily timescales for organisms that undergo diel vertical migration. Krill are
355 successful in highly variable environments through a variety of strategies, including the capacity
356 for negative growth rates, which are commonly observed (~25 % of the time) in juvenile and
357 adult krill year-round (Shaw et al., 2010). Potential dependence of AARS activity on sufficient
358 (non-starvation) food conditions makes the timing of sampling an important consideration for
359 field studies. These mature female krill were likely investing significant energy into reproductive
360 output rather than somatic growth, which could potentially decouple spAARS and IGR.
361 However, other studies have shown that spAARS activity and copepod egg production rates are
362 correlated in the laboratory (Holmborn et al., 2009) and in the field (Yebra et al., 2005). The
363 influence of food availability on the relationship between spAARS activity and growth rate is
364 difficult to evaluate currently because there are few studies at low food concentrations (Herrera,
365 2014), but deserves further investigation.
366 The IGR-estimated growth rates we measured under the low-food conditions
367 conventionally used for IGR are within the usual range for individuals of this size (Shaw et al.,

2010), although the range we observed is slightly narrower, as would be expected from the narrow spatiotemporal coverage of our sampling. Size specific growth rate of animals generally decreases with increasing body size, as has been previously observed in *E. pacifica* (Shaw et al., 2010), and seen in our IGR data. The positive relationship between log(spAARS) and post-molt total length was the factor that best explained spAARS activity. However, total length did not explain much of the variability in spAARS, as evidenced by the low R^2 value. AARS activity has not been published for this species before, but our spAARS values are similar to those of *E. distinguenda* in the Eastern Tropical Pacific (Herrera et al., 2019). It is likely that IGR and AARS do not index growth over identical periods prior to measurement, as enzyme indices give a snap-shot image of the metabolic state of organisms and IGR reflects increases in size over the molt cycle. Although very few data were available, comparing AARS of individuals that were frozen immediately without an incubation period to IGR of individuals from the same location did not improve the relationship between the two. Further constraining the timescales over which they integrate would increase the utility and improve interpretation of these methods.

We observed significant activity in all NADH Blanks, indicating that the AARS assay may be measuring other processes in addition to PPi-producing reactions. The best model of NADH Blank activity included Assay activity and ETS activity, however, three other models had AICc scores within 2 of the best model and one of those only included Assay activity, indicating that ETS activity did not significantly improve the fit of the model. The oxidation in the NADH Blank could be driven by other enzymes in the protein synthesis pathway, giving rise to the relationship between blank and assay activity. Another potential process contributing to NADH oxidation comes from microbial enzymes released from within or on the krill during homogenization. Although outside the scope of this study, assay conditions, e.g., pH, could be

391 optimized to minimize possible contribution of prokaryotic enzymes, and a new blank method
392 could improve the specificity of this assay. It is also important to note that the AARS assay is not
393 a traditional enzyme assay as it is meant to measure the activity of many different AARS
394 enzymes at the same time, and it does not include the addition of saturating substrates to measure
395 the maximum rate of reaction (Vmax). The close correlation between the NADH Blank and the
396 AARS assay may be due to similar substrate limitation in the reactions affecting each. How
397 variations in substrate concentrations influence AARS activity measurements is an important
398 area for future research. We are unable to evaluate whether correcting the assay activity with the
399 NADH Blank improves its relationship with growth rate using our data due to the differences
400 between the two methods described above. However, correlations between spAARS activity and
401 environmental drivers increased when spAARS was corrected using the NADH Blank
402 (McLaskey 2019; McLaskey and Keister, *unpublished*), indicating that it may be eliminating
403 noise from the assay signal. Nevertheless, as with all enzyme activities, a calibration is needed
404 between the enzyme activity and growth rate of the organisms assessed by direct methods (Yebra
405 et al. 2017). Therefore, testing whether the use of this blank improves the relationship between
406 AARS activity and growth rate of zooplankton would be an important next step in the
407 development of this method.
408

409 # 5. Conclusions

410 Estimating zooplankton growth and production rates remains a significant challenge in
411 zooplankton ecology but is advancing through the development of biochemical assays.
412 Intercomparison of these assays is needed to assess the advantages and limitations of different
413 methods. IGR and AARS activity index krill responses over different timescales and care should

be exercised when applying either as a metric of population growth rate when measured infrequently or among few individuals. IGR estimates weight from length measurements, which are determined over the course of the molt cycle. AARS activity can track short-term variations in environmental experience and therefore be useful as a high-resolution index of protein synthesis. The results of our NADH Blank indicate that the AARS assay is measuring processes in addition to aminoacylation, which may be contributing additional variability, and its further study would provide a potential path to improve the specificity of the AARS assay.

Acknowledgements

We are grateful to Ted Packard and May Gómez for guidance on the ETS activity methods; Akash Sastri for helpful discussion about the data; Jodi Young for discussion about enzyme activities; Captain Ken Pinnell, Brian Bare, and Jen Nomura of the R/V Clifford A. Barnes for field sampling; Amanda Winans, Katie Keil, Anna Boyar, Anita Montero, and Morgan Beste for help in the field; and Shelly Carpenter and Rachel Lundeen for practical advice on running assays.

Funding: This research was supported by the Washington Ocean Acidification Center, the University of Washington School of Oceanography, the National Science Foundation (NSF) Graduate Research Fellowship Program under Grant No. DGE-1256082 (AKM), and NSF award OCE-1657992 to JEK.

Supporting Information

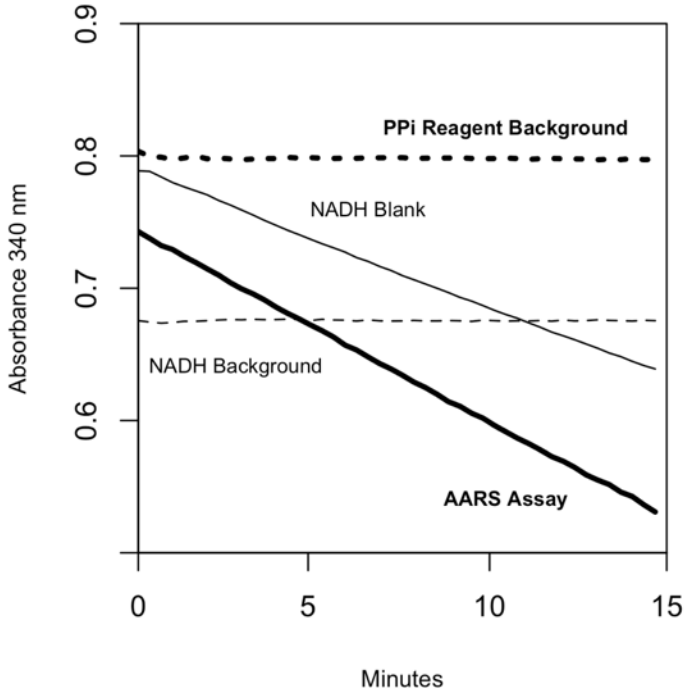

S1 Figure. Example AARS Assay (thick line), NADH Blank (thin line), PPi Reagent Background blank (dashed thick line), and NADH Background blank (dashed thin line) for one sample showing the change in absorbance over time.

443 S1 Table. AICc scores for linear models of IGR-estimated growth rate (d^{-1}) and spAARS activity
444 after undergoing a log(y) transformation. Best models indicated in bold.

	Response		
Model Structure	Growth Rate	log(spAARS)	Growth Increment
Response= Protein + intercept	-315.6	58.2	-1.4
Response= Length + intercept	-325.3	**53.9**	**-7.0**
Response= DW + intercept	-322.6	54.4	-4.1
Response= Time + intercept	-310.5	60.4	2.5
Response= Temp + intercept	-311.5	60.8	3.1
Response= Chl + intercept	-317.1	59.8	3.5
Response= Length + Chl + intercept	-328.7	**52.1**	-4.7
Response= Length + Temp + intercept	-323.0	**53.3**	-4.7
Response= Length + Time + intercept	-328.0	55.7	**-7.9**
Response= Length + Protein + intercept	-324.5	55.0	-5.2
Response= Length + Temp + Time + intercept	-325.5	54.6	-5.6
Response= Length + Chl + Time + intercept	**-331.6**	**53.8**	-5.5

445

446

447 S2 Table. AICc scores for linear mixed models of investigating the effect of IGR incubation on
448 spAARS activity after undergoing a log(y) transformation and spETS activity. In the models,
449 fixed effects are shown without parentheses and random effects with parentheses. Best models
450 indicated in bold.

	Response	
Model Structure	log(spAARS)	spETS
Response= (station) + intercept	70	**-185.5**
Response= Before/After + (station) + intercept	**67.9**	-177.5
Response= Before/After * (station) + intercept	67.9	-177.5

451

452

S3 Table. AICc scores for linear models of change in absorbance in the NADH Blank, after undergoing a log transform. Best models indicated in bold.

Model Structure	AICc
log(NADH Blank) = station + intercept	280.3
log(NADH Blank) = dry weight + intercept	239.8
log(NADH Blank) = log(Assay) + intercept	**107.0**
log(NADH Blank) = ETS + intercept	261.9
log(NADH Blank) = dry weight + log(Assay) + intercept	**106.7**
log(NADH Blank) = log(Assay) + ETS + intercept	**105.0**
log(NADH Blank) = dry weight + ETS + intercept	240.2
log(NADH Blank) = log(Assay) + station + intercept	121.7
log(NADH Blank) = dry weight + station + intercept	231.2
log(NADH Blank) = log(Assay) + ETS + station + intercept	120.8
log(NADH Blank) = dry weight + ETS + station + intercept	232.2
log(NADH Blank) = dry weight + log(Assay) + ETS + intercept	**107.0**
log(NADH Blank) = dry weight + log(Assay) + station + intercept	122.0
log(NADH Blank) = dry weight + log(Assay) + ETS + station + intercept	123.3

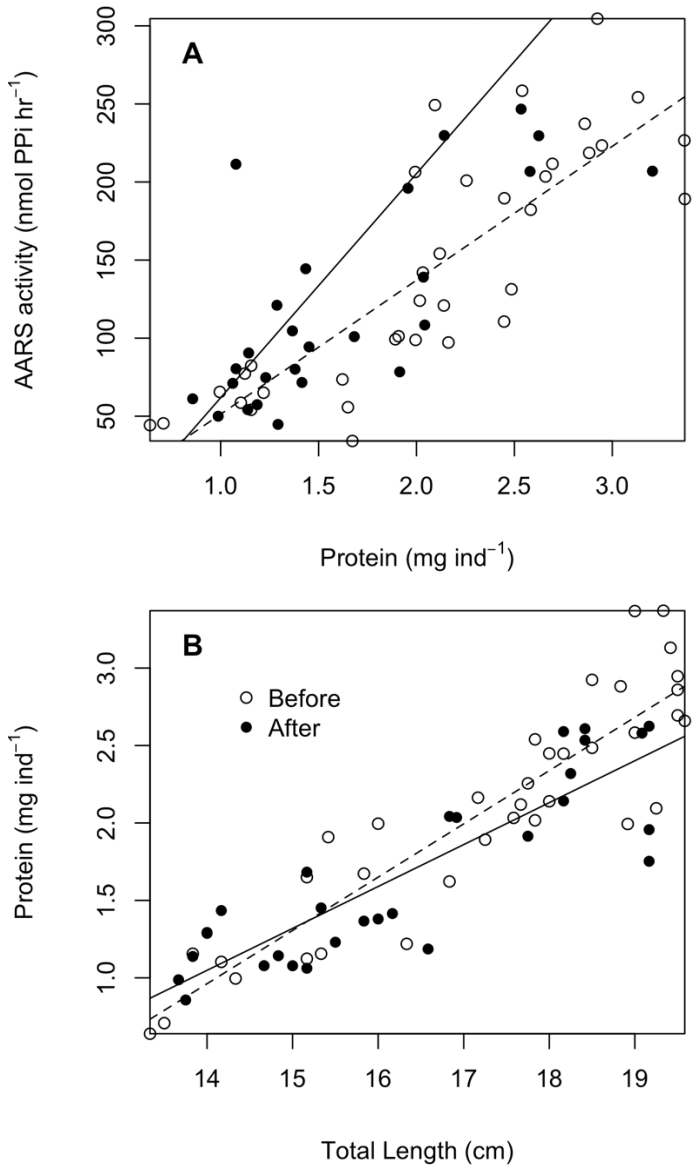

S2 Figure. Correlations of measurements from individual krill incubated in IGR experiments (solid points and solid line) and individuals immediately frozen in the field (open circles and dashed line). (A) AARS activity (nmol PPi ind-1 hr-1) versus assayed protein content (After Incubation $p<0.0001$, $R^2=0.50$; Before Incubation $p<0.0001$, $R^2=0.68$) and (B) protein content (mg ind^{-1}) versus measured total length (After $p<0.0001$, $R^2=0.78$; Before $p<0.0001$, $R^2=0.81$).

References

Atkinson, A., Shreeve, R.S., Hirst, A.G., Rothery, P., Tarling, G.A., Pond, D.W., Korb, R.E., Murphy, E.J., Watkins, J.L., 2006. Natural growth rates in Antarctic krill (*Euphausia superba*): II. Predictive models based on food, temperature, body length, sex, and maturity stage. Limnol. Oceanogr. 51, 973–987. https://doi.org/10.4319/lo.2006.51.2.0973

Awai, T., Ichihashi, N., Yomo, T., 2015. Activities of 20 aminoacyl-tRNA synthetases expressed in a reconstituted translation system in *Escherichia coli*. Biochem. Biophys. Reports 3, 140–143. https://doi.org/10.1016/j.bbrep.2015.08.006

Boniecki, M.T., Vu, M.T., Betha, A.K., Martinis, S.A., 2008. CP1-dependent partitioning of pretransfer and posttransfer editing in leucyl-tRNA synthetase. Proc. Natl. Acad. Sci. 105, 19223–19228. https://doi.org/10.1073/pnas.0809336105

Chang, G., Pan, F., Lin, Y., Wang, H., 1984. Continuous spectrophotometric assay for aminoacyl-tRNA synthetases. Anal. Biochem. 142, 369–372. https://doi.org/10.1016/0003-2697(84)90478-0

Feinberg, L.R., Shaw, C.T., Peterson, W.T., 2007. Long-term laboratory observations of *Euphausia pacifica* fecundity: comparison of two geographic regions. Mar. Ecol. Prog. Ser. 341, 141–152. https://doi.org/10.3354/meps341141

Gómez, M., Torres, S., Hernández-León, S., 1996. Modification of the electron transport system (ETS) method for routine measurements of respiratory rates of zooplankton. South African J. Mar. Sci. 17, 15–20. https://doi.org/10.2989/025776196784158446

Guerra, C., 2006. Bestimmung von Wachstumsraten bei larvalem Krill (*Euphausia superba*) im

485 antarktischen Herbst in der Lazarev-See —Ein Vergleich verschiedener methodischer
486 Ansaätze. Diplom thesis, Universität Bremen.
487 Herrera, I., 2014. The use of AARS activity as a proxy for zooplankton and ichthyoplankton
488 growth rates. PhD Thesis, University of Las Palmas de Gran Canaria.
489 https://accedacris.ulpgc.es/handle/10553/12495
490 Herrera, I., López-Cancio, J., Yebra, L., Hernández-Léon, S., 2017. The effect of a strong warm
491 winter on subtropical zooplankton biomass and metabolism. J. Mar. Res. 75, 557–577.
492 https://doi.org/10.1357/002224017822109523
493 Herrera, I., Yebra, L., Antezana, T., Giraldo, A., Färber-Lorda, J., Hernández-León, S., 2019.
494 Vertical variability of *Euphausia distinguenda* metabolic rates during diel migration into
495 the oxygen minimum zone of the Eastern Tropical Pacific off Mexico. J. Plankton Res. 41,
496 165–176. https://doi.org/10.1093/plankt/fbz004
497 Herrera, I., Yebra, L., Hernández-Léon, S., 2012. Effect of temperature and food concentration
498 on the relationship between growth and AARS activity in *Paracartia grani* nauplii. J. Exp.
499 Mar. Bio. Ecol. 416, 101–109. https://doi.org/10.1016/j.jembe.2012.02.019
500 Holmborn, T., Dahlgren, K., Holeton, C., Hogfors, H., Gorokhova, E., 2009. Biochemical proxies
501 for growth and metabolism in *Acartia bifilosa* (Copepoda, Calanoida). Limnol. Oceanogr.
502 Methods 7, 785–794. https://doi.org/10.4319/lom.2009.7.785
503 Ikeda, T., 1977. The effect of laboratory conditions on the extrapolation of experimental
504 measurements to the ecology of marine zooplankton. IV. Changes in respiration and
505 excretion rates of boreal zooplankton species maintained under fed and starved
506 conditions. Mar. Biol. 41, 241–252. https://doi.org/10.1007/BF00394910

Kobari, T., Sastri, A.R., Yebra, L., Liu, H., Hopcroft, R.R., 2019. Evaluation of trade-offs in traditional methodologies for measuring metazooplankton growth rates: Assumptions, advantages and disadvantages for field applications. Prog. Oceanogr. 178, 102137. https://doi.org/10.1016/J.POCEAN.2019.102137

Mauchline, J., and Fisher, L.R., 1969. The biology of the euphausiids. Adv. Mar. Biol. 7, 1–454.

McLaskey, A.K., 2019. Multiple effects of ocean change on crustacean zooplankton: A coupled field-laboratory approach. PhD Thesis, University of Washington. http://hdl.handle.net/1773/44416

McKinnon, A.D., Doyle, J., Duggan, S., Logan, M., Lønborg, C., Brinkman, R., 2015. Zooplankton Growth, Respiration and Grazing on the Australian Margins of the Tropical Indian and Pacific Oceans. PLoS One 10, e0140012. https://doi.org/10.1371/journal.pone.0140012

Nicol, S., 2000. Understanding krill growth and aging: the contribution of experimental studies. Can. J. Fish. Aquat. Sci. 57, 168–177. https://doi.org/10.1139/f00-173

Nicol, S., Stolp, M., Cochran, T., Geijsel, P., Marshall, J., 1992. Growth and shrinkage of Antarctic krill *Euphausia superba* from the Indian Ocean sector of the Southern Ocean during summer. Mar. Ecol. Prog. Ser. 89, 175–181. https://doi.org/10.3354/meps089175

Owens, T.G., King, F.D., 1975. The measurement of respiratory electron-transport-system activity in marine zooplankton. Mar. Biol. 30, 27–36. https://doi.org/10.1007/BF00393750

Packard, T.T., Christensen, J.P., 2004. Respiration and vertical carbon flux in the Gulf of Maine water column. J. Mar. Res. 62, 93–115. https://doi.org/10.1357/00222400460744636

Packard, T.T., Devol, A.H., King, F.D., 1975. The effect of temperature on the respiratory

electron transport system in marine plankton. Deep Sea Res. Oceanogr. Abstr. 22, 237–249. https://doi.org/10.1016/0011-7471(75)90029-7

Packard, T.T., Williams, B., 1981. Rates of respiratory oxygen consumption and electron transport in surface seawater from the northwest Atlantic. Oceanol. acta 4, 351–358.

Pinchuk, A.I., Hopcroft, R.R., 2007. Seasonal variations in the growth rates of euphausiids (*Thysanoessa inermis*, *T. spinifera*, and *Euphausia pacifica*) from the northern Gulf of Alaska. Mar. Biol. 151, 257–269. https://doi.org/10.1007/s00227-006-0483-1

Quetin, L.B., Ross, R.M., 1991. Behavioral and Physiological Characteristics of the Antarctic Krill, *Euphausia superba*. Am. Zool. 31, 49–63. https://doi.org/10.1093/icb/31.1.49

Ross, R.M., Quetin, L.B., Baker, K.S., Vernet, M., Smith, R.C., 2000. Growth limitation in young *Euphausia superba* under field conditions. Limnol. Oceanogr. 45, 31–43. https://doi.org/10.4319/lo.2000.45.1.0031

Shaw, C.T., Peterson, W.T., Feinberg, L.R., 2010. Growth of *Euphausia pacifica* in the upwelling zone off the Oregon coast. Deep Sea Res. Part II Top. Stud. Oceanogr. 57, 584–593. https://doi.org/10.1016/J.DSR2.2009.10.008

Smith, P.K., Krohn, R.I., Hermanson, G.T., Mallia, A.K., Gartner, F.H., Provenzano, M.D., Fujimoto, E.K., Goeke, N.M., Olson, B.J., Klenk, D.C., 1985. Measurement of protein using bicinchoninic acid. Anal. Biochem. 150, 76–85.

Tarling, G.A., Shreeve, R.S., Hirst, A.G., Atkinson, A., Pond, D.W., Murphy, E.J., Watkins, J.L., 2006. Natural growth rates in Antarctic krill (*Euphausia superba*): I. Improving methodology and predicting intermolt period. Limnol. Oceanogr. 51, 959–972. https://doi.org/10.4319/lo.2006.51.2.0959

551 Yebra, L., Berdalet, E., Almeda, R., Pérez, V., Calbet, A., Saiz, E., 2011. Protein and nucleic acid
552 metabolism as proxies for growth and fitness of *Oithona davisae* (Copepoda,
553 Cyclopoida) early developmental stages. J. Exp. Mar. Bio. Ecol. 406, 87–94.
554 https://doi.org/10.1016/j.jembe.2011.06.019
555 Yebra, L., Harris, R.P., Smith, T., 2005. Comparison of five methods for estimating growth of
556 *Calanus helgolandicus* later developmental stages (CV-CVI). Mar. Biol. 147, 1367–1375.
557 https://doi.org/10.1007/s00227-005-0039-9
558 Yebra, L., Hernández-León, S., 2004. Aminoacyl-tRNA synthetases activity as a growth index in
559 zooplankton. J. Plankton Res. 26, 351–356. https://doi.org/10.1093/plankt/fbh028
560 Yebra, L., Hirst, A.G., Hernandez-Leon, S., Harris, R.P., 2006. Assessment of *Calanus*
561 *finmarchicus* growth and dormancy using the aminoacyl-tRNA synthetases method. J.
562 Plankton Res. 28, 1191–1198. https://doi.org/10.1093/plankt/fbl049
563 Yebra, L., Kobari, T., Sastri, A.R., Gusmão, F., Hernández-León, S., 2017. Advances in Biochemical
564 Indices of Zooplankton Production. Adv. Mar. Biol. 76, 157–240.
565 https://doi.org/10.1016/BS.AMB.2016.09.001
566

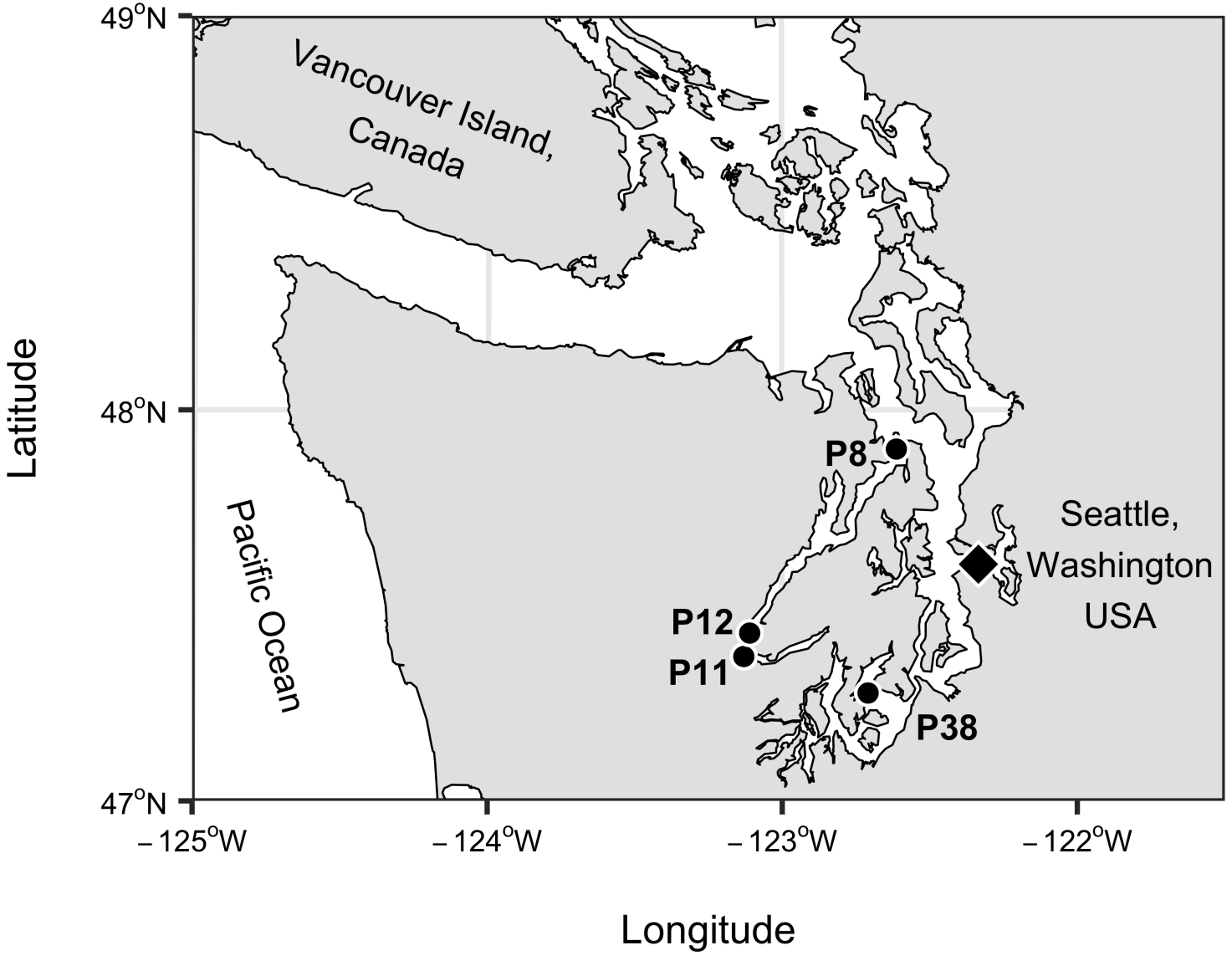
49°N
48°N
47°N
Latitude
– 125°W
– 124°W
– 123°W
– 122°W
Longitude
Vancouver Island,
Canada
Pacific Ocean
P8
P12
P11
P38
Seattle,
Washington
USA

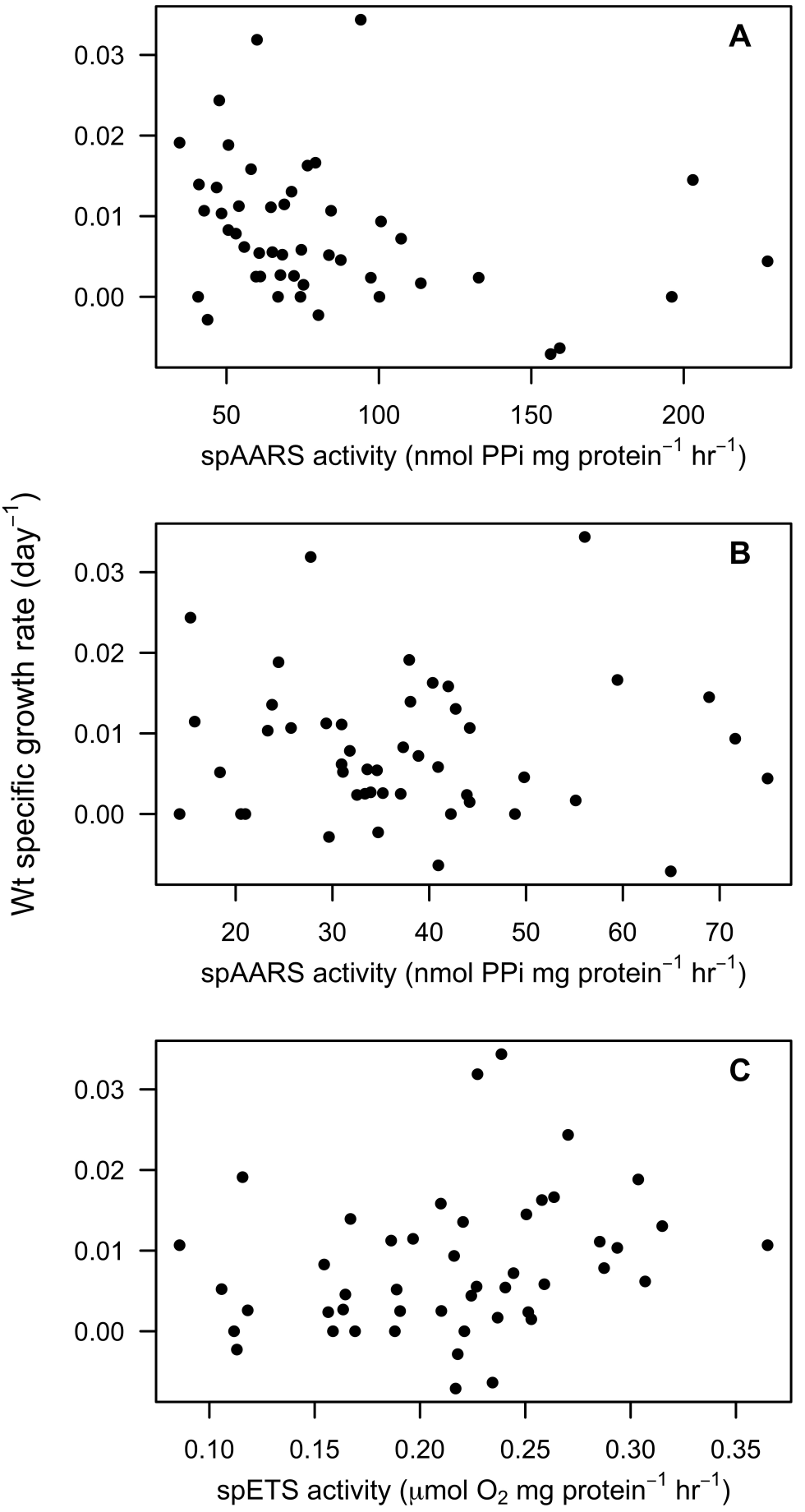
A
B
C
0.03
0.02
0.01
0.00
50
100
150
200
20
30
40
50
60
70
0.10
0.15
0.20
0.25
0.30
0.35
Wt specific growth rate (day^{-1})
spAARS activity (nmol PPi mg protein^{-1} hr^{-1})
spAARS activity (nmol PPi mg protein^{-1} hr^{-1})
spETS activity (μmol O_2 mg protein^{-1} hr^{-1})

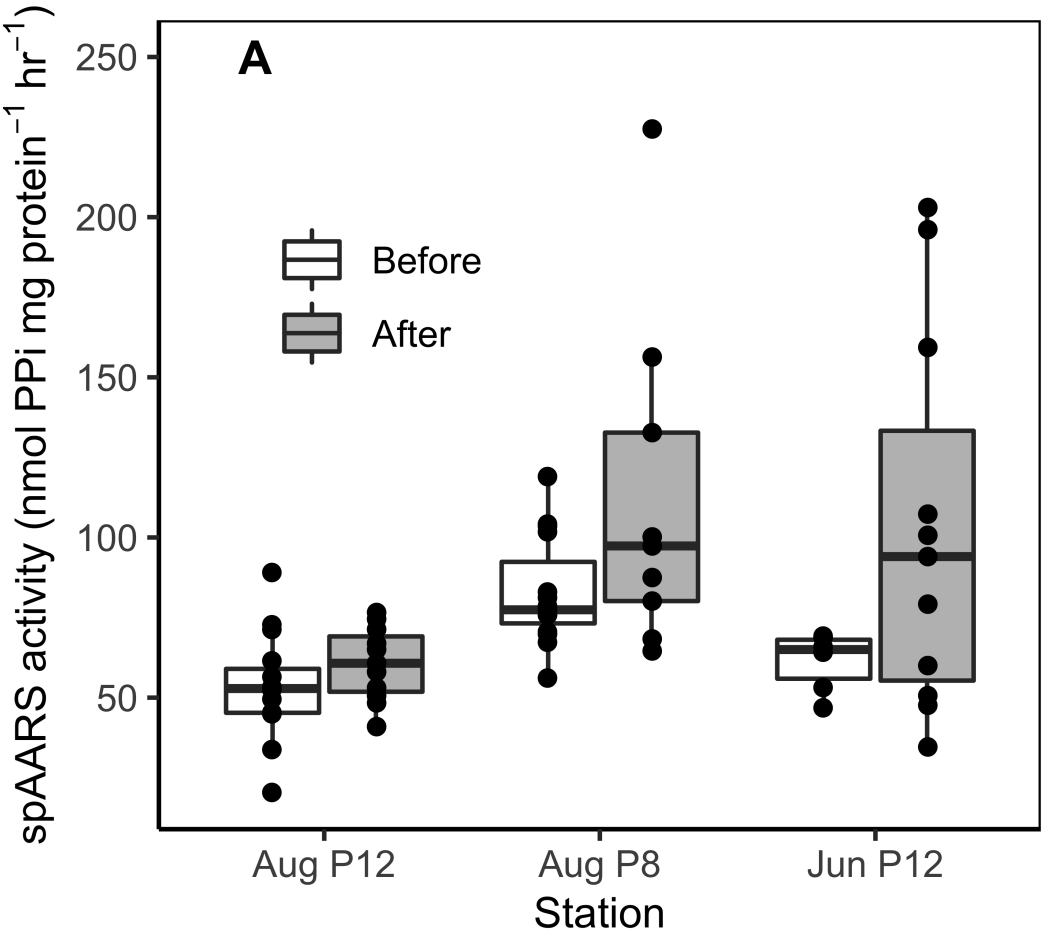
A
Before
After
spAARS activity (nmol PPi mg protein^{-1} hr^{-1})
250
200
150
100
50
Aug P12
Aug P8
Jun P12
Station

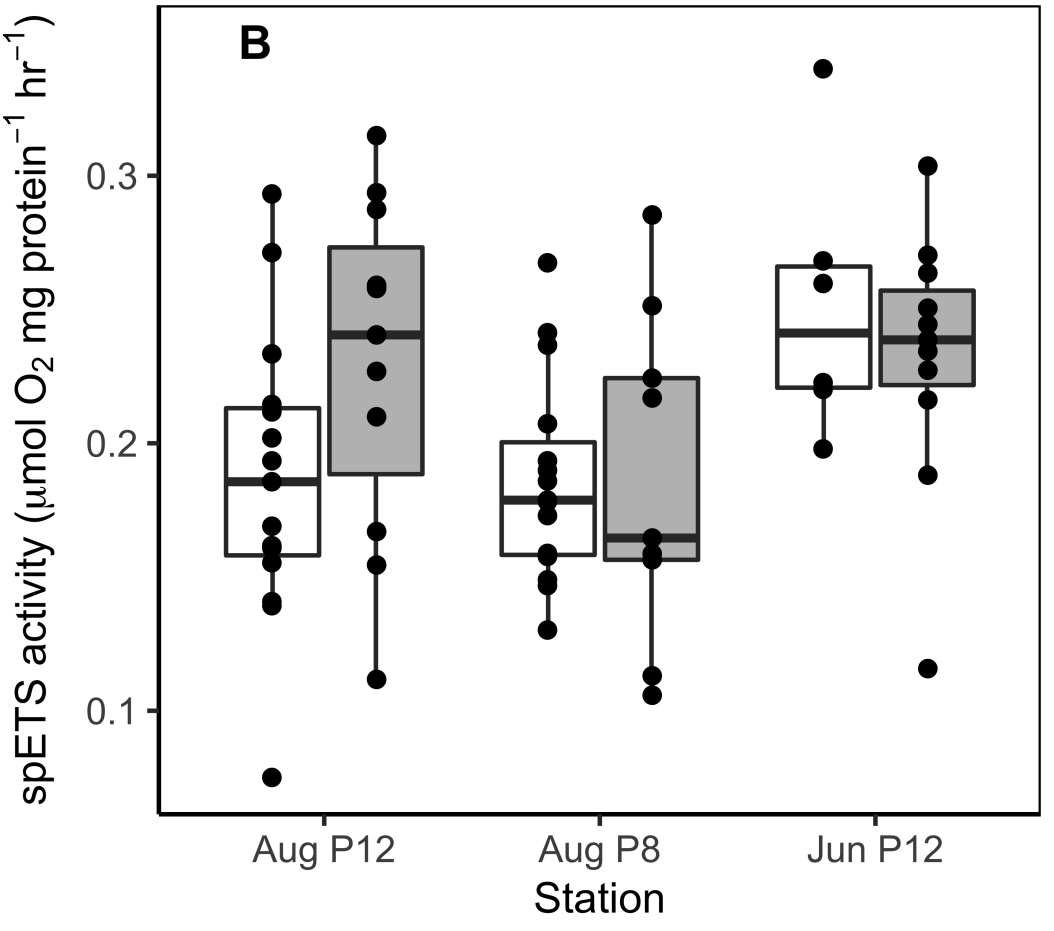
B
spETS activity (μmol O_2 mg protein^{-1} hr^{-1})
0.3
0.2
0.1
Aug P12
Aug P8
Jun P12
Station

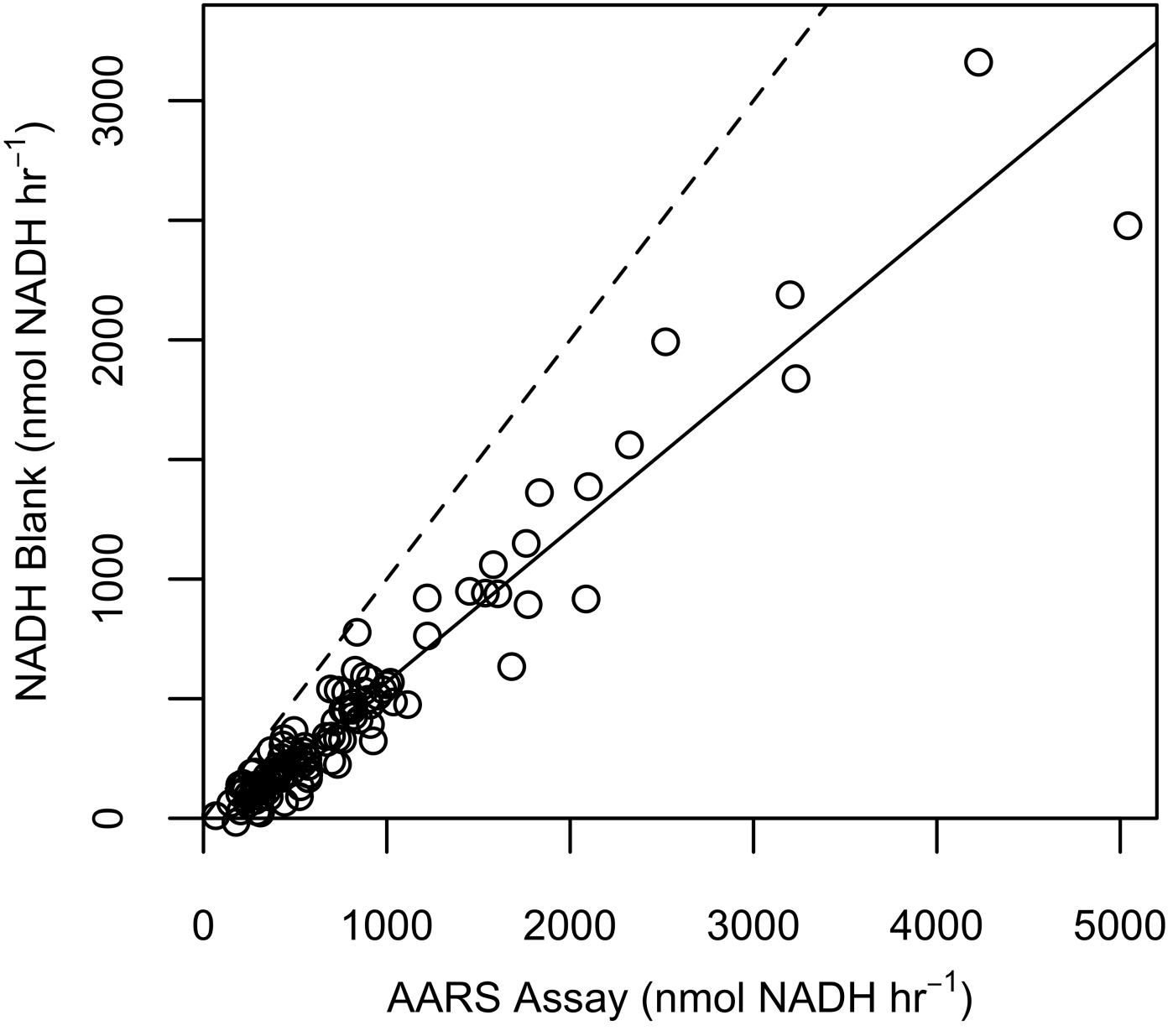
NADH Blank (nmol NADH hr^{-1})
0
1000
2000
3000
0
1000
2000
3000
4000
5000
AARS Assay (nmol NADH hr^{-1})